

Studies on thermal and mechanical properties of polyimide–clay nanocomposites

T. Agag¹, T. Koga, T. Takeichi*

School of Materials Science, Toyohashi University of Technology, Tempaku-cho, Toyohashi 441-8580, Japan

Received 16 August 2000; received in revised form 16 October 2000; accepted 25 October 2000

Abstract

Nanocomposites from polyimide and clay were prepared aiming at finding a promising method for enhancing particularly the tensile modulus of polyimide films. Polyimide–clay hybrids were prepared by blending of poly(amide acid) and organically modified-montmorillonite (OMMT) as a type of layered clays. Poly(amide acid) was prepared from the reaction of 3,3',4,4'-biphenyltetracarboxylic dianhydride (BPDA) and *p*-phenylenediamine (PDA). Also, poly(amide acid) from pyromellitic dianhydride (PMDA) and 4,4'-oxydianiline (ODA) was prepared for comparison. OMMT was prepared by surface treatment of montmorillonite (MMT) with ammonium chloride salt of 12-aminolauric acid. XRD indicated that the OMMT layers were exfoliated and dispersed into the poly(amide acid) and polyimide film. Tensile properties measurements of polyimide–clay hybrids indicated that the addition of 2 wt.% of OMMT increased the tensile modulus of BPDA/PDA polyimide up to 12.1 GPa, which is ca. 42% higher than the pristine BPDA/PDA polyimide. Tensile modulus of PMDA/ODA also increased up to 6.2 GPa, which is ca. 110% higher than that of the original PMDA/ODA polyimide. The glass transition temperatures of the BPDA/PDA nanocomposites were higher than that of the original polyimide. The thermal expansion coefficient of the BPDA/PDA polyimide film decreased by the inclusion of clay. Isothermal and dynamic TGA showed that the both types of polyimide nanocomposites have higher decomposition temperatures in comparison with the original polyimides. © 2001 Elsevier Science Ltd. All rights reserved.

Keywords: Polyimide; Montmorillonite; Polyimide–clay hybrids

1. Introduction

The mechanical and thermal properties of polymers are generally improved by the addition of inorganic additives. The challenges in this area of high performance organic–inorganic hybrid materials are to obtain significant improvements in the interfacial adhesion between the polymer matrix and the reinforcing material since the organic matrix is relatively incompatible with the inorganic phase. Generally, a better interfacial bonding will impart better properties to a polymer composite such as high modulus, tensile strength, and hardness as well as resistance to tear, fatigue, cracking and corrosion [1,2].

Nanocomposite is a class of composites in which the reinforcing phase dimensions are in the order of nanometers [3,4]. Because of their nanometer size characteristics, nanocomposites possess superior properties than the conventional microcomposites due to maximizing the

interfacial adhesion. Nanostructured composites based on polymer and layered silicates typically exhibit properties far superior to those of separate components, which make them extremely interesting in the field of design and creation of new construction materials [4–6]. Thus, smectite clays as layered silicates are considered to be good candidates for the preparation of organic–inorganic nanocomposites because they can be broken down into nanoscale building blocks resulting often in optically transparent hybrids. In the last decade, the properties of a variety of elastomers [7,8], linear [9,10] or crosslinked [11–13] polymers have been improved by the incorporation of layered silicates. Several studies revealed that the inclusion of clay minerals enhanced the mechanical properties of both rigid and flexible polymer systems [14,15].

Polyimides are considered to be one of the most important super-engineering materials because of their superior mechanical properties at elevated temperature due to their thermal stability [16,17]. Electronic industry is the typical extensive applications of polyimides including interlayer insulation films, buffer coating films, alpha-ray shielding films, and alignment films for liquid crystal

* Corresponding author. Tel.: +81-532-44-6815; fax: +81-532-48-5833.

E-mail address: takeichi@tutms.tut.ac.jp (T. Takeichi).

¹ On leave from the University of Tanta, Tanta, Egypt.

displays [18]. Study on tensile properties is very important for such kind of applications. It is known that the tensile modulus of rigid rod polyimides such as 3,3',4,4'-biphenyl-tetracarboxylic dianhydride (BPDA)/*p*-phenylenediamine (PDA) and pyromellitic dianhydride (PMDA)/PDA is much higher than that of flexible or semi-flexible polyimides such as BPDA/4,4'-Oxydianiline (ODA) and PMDA/ODA. Higher modulus can be obtained for rigid rod polyimide films by either cold drawing of poly(amide acid) precursor [19–23] or delacoholization at imidization of poly(amide ester)s [24–26].

Recently, polyimide–clay hybrids have been studied [27–31]. Those studies on polyimide–clay nanocomposites were mainly directed towards elucidating the effect of inclusion of clay on the barrier properties and linear coefficient of thermal expansion (CTE) of the polyimide films. The gas permeability of the polyimide–clay nanocomposites lowered in compare with the pristine polyimide [27,28]. Also, the incorporation of the clay into polyimide film has obviously lowered the CTE [29,30]. But, little has been studied on the effect of clay on the mechanical properties of polyimide except some viscoelastic analyses for the Kapton type polyimide [29]. It is expected that the dispersion of the clay nanolayers mainly along the film plane could improve the tensile modulus of polyimide, thus giving a novel and easy method for enhancing the tensile modulus of polyimide film. Rigid rod BPDA/PDA is a unique type of polyimide because of its high modulus and low CTE. Also, BPDA/PDA has unique features such as remarkable spontaneous in-plane orientation and the sharp increase in the tensile modulus by cold drawing. On the other hand, PMDA/ODA does not show such remarkable features due to the presence of flexibilizing ether units in the main chain. All the previous studies on polyimide–clay nanocomposites were focused on the Kapton type polyimide and there are no reports on the BPDA/PDA nanocomposites. Due to the outstanding properties, BPDA/PDA films are widely used in micro-electronic and aerospace industries. Since the properties of rigid BPDA/PDA is completely different from the flexible PMDA/ODA, it is worth studying the effect of the inclusion of the clay nanolayer on the mechanical properties especially tensile properties as well as thermal properties for BPDA/PDA. The effect will also be studied for the Kapton type polyimide because little has been reported in the previous studies [27,29] on the tensile properties for the Kapton-type polyimide–clay hybrids.

2. Experimental

2.1. Reagents

Kunipia-F, kindly supplied by Kunimine Ind. Co., is a Na⁺-montmorillonite (MMT) with cation exchange capacity (CEC) of 119 meq/100 g. 12-Aminolauric acid

was used as received from Tokyo Chemical Industry. PDA was received from Tokyo Chemical Industry and purified by repeated sublimation. BPDA was recrystallized from acetic anhydride followed by sublimation. PMDA was purified firstly by recrystallization from acetic anhydride and then by sublimation. ODA was purified by sublimation. *N,N*-dimethylacetamide (DMAc) was dried by distillation under reduced pressure over sodium hydride.

2.2. Preparation of organically modified montmorillonite

Organophilic montmorillonite (OMMT) was prepared from MMT by ion exchange reaction using ammonium chloride salt of 12-aminolauric acid in water according to the reported method [27]. The amount of ammonium salt of aminolauric acid grafted onto the MMT surfaces was calculated to be 20.8% based on the total charge on the MMT layers.

A suspension of OMMT in DMAc was prepared by dispersion of 3.77 g of OMMT in 96.23 g of DMAc by heating at 80°C for 2 h. A stable suspension was obtained and kept until use.

2.3. Preparation of poly(amide acid)

Poly(amide acid) from BPDA and PDA was prepared as follows: Into a 200 ml flask equipped with nitrogen inlet and mechanical stirrer, PDA (20.00 mmol, 2.1628 g) and DMAc (130 g) were placed. The mixture was stirred until getting clear solution. Equimolar amount of solid BPDA (20.00 mmol, 5.8844 g) was added in one batch to the PDA solution and the wall of the flask was washed with 9.72 g of DMAc. The reaction mixture was stirred for 10 h at room temperature to give a transparent yellow viscous solution of 5.45 wt.% of poly(amide acid). The poly(amide acid) solution was kept in a freezer until use. The inherent viscosity of the poly(amide acid) was 2.20 dl/g (0.5 g/dl in NMP at 30°C).

Poly(amide acid) for the Kapton type polyimide was prepared similarly to the above method. The poly(amide acid) solution was also kept in a freezer until use. The inherent viscosity of the Kapton type poly(amide acid) was 1.13 dl/g (0.5 g/dl in NMP at 30°C).

2.4. Preparation of polyimide–clay hybrids

The polyimide–clay hybrids were prepared by blending the required ratios of OMMT suspension in DMAc with poly(amide acid) in DMAc. The blends were stirred for 5 h to achieve complete dispersion of OMMT into poly(amide acid). The blends were cast on glass plates, dried in an air convection oven at 60°C for 5 h, cured at 150, 200 and 250°C for 1 h each, and postcured in air oven at 300 and 350°C for 1 h each, as fixed on the substrates, to obtain yellow colored transparent films.

2.5. Cold drawing of BPDA/PDA poly(amide acid)–OMMT hybrid films

Some BPDA/PDA poly(amide acid)–OMMT hybrid films were peeled from the glass substrate after drying at 60°C for 5 h and then were cut into 20 mm × 30 mm strips. The strips were uniaxially drawn with a crosshead speed of 1 mm/min using films of 3 cm long [23]. The appropriately drawn films were kept fixed under tension for 5 h at r.t., and then cured according to the previously mentioned thermal schedule.

2.6. Measurements

IR spectra were obtained with JASCO spectrophotometer model FT/IR-420. Differential scanning calorimetry (DSC) was recorded using Rigaku Thermo Plus 2 DSC8230 at a heating rate of 10°C/min under nitrogen. Dynamic thermogravimetric analysis (TGA) was performed with Rigaku Thermo Plus 2 TG-DTA TG8120 at a heating rate of 5°C/min under argon. Isothermal TGA was carried out by Rigaku Thermo Plus 2 TG-DTA TG8120 by heating the samples (ca. 5 mg) at 500°C for 3 h. Dynamic viscoelastic measurements were conducted on ORIENTEC Automatic Dynamic Viscoelastomer Rheovibron model DDV-01FP at 35 Hz at a heating rate of 4°C/min. Tensile properties were recorded with Imada Seisaku-sho Model SV-3 at a crosshead speed of 1 mm/min using films of 2 cm long. The tensile properties of each sample were determined from an average of at least five tests. XRD was measured in reflection mode using a X-ray diffractometer, Rigaku, RINT2000 using CuK α radiation. The scanning rate was 0.3°/min from $2\theta = 2$ to 10 and 2°/min from $2\theta = 10$ to 40.

3. Results and discussion

3.1. Preparation of polyimide–clay hybrid nanocomposites

In order to disperse the hydrophilic MMT well into organic polymers, Na ions on its surface should be exchanged by organic cations through ion exchange process to render the surface hydrophobic [6]. Thus, there will be hydrophobic environment into the clay galleries to accommodate the hydrophobic poly(amide acid). In polyimide clay system, many aliphatic surfactants and aromatic diamines as well as amino acids have been studied for the surface modification of MMT to prepare an OMMT [27,30]. In this study, we used ammonium salt of 12-aminolauric acid for ion exchanging of the Na⁺ ions on the MMT surfaces, expecting that the presence of carboxyl groups may enhance the interaction between OMMT and poly(amide acid) through hydrogen bonding. X-ray diffraction (XRD) measurements (Fig. 1) showed that the interlayer spacing of MMT ($2\theta = 7.12$, $d = 1.24$ nm) was increased after surface treatment with ammonium chloride

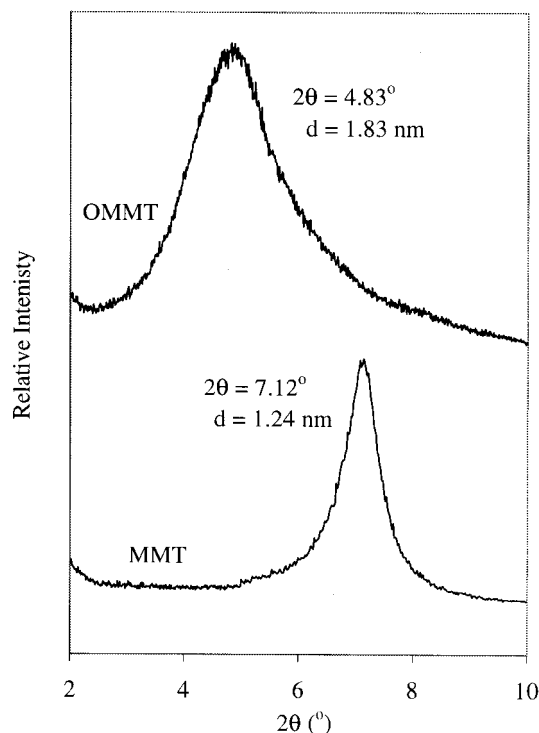


Fig. 1. XRD patterns of MMT and OMMT.

salt of 12-aminolauric acid to afford OMMT ($2\theta = 4.83$, $d = 1.83$ nm).

BPDA/PDA poly(amide acid) was blended with different weight ratios of OMMT. We generally prepared poly(amide acid) in 10 wt.% solution which was too viscous to get homogeneous blend. Therefore, we found that poly(amide acid) in ca. 5 wt.% is suitable to get homogenous blend. Hereafter, poly(amide acid) of BPDA/PDA is abbreviated as PAA and its polyimide as PI, and the number next to the name is referring to the OMMT content. The cast films after drying were cured at 150, 200, 250, 300 and 350°C for 1 h each in the air atmosphere. The thickness of the resulted hybrid nanocomposite films was ca. 30 μ m. The films were quite transparent for hybrids with clay loading up to 4 wt.%. The films, however, became translucent with the increase of the OMMT content for more than 4%. The transparency of the hybrid nanocomposites comes from the dispersion of the clay nanolayer into the polyimide film. The clay particles, at high clay content, could not be completely dispersed into nanolayer and some remained as aggregates, which reduce the transparency of the visible light [27].

Preparation of PMDA/ODA polyimide–clay nanocomposites was performed similarly. The films were transparent as in the case of BPDA/PDA nanocomposites.

3.2. Curing behavior of polyimide–clay hybrid nanocomposites

The effect of the inclusion of OMMT on the imidization

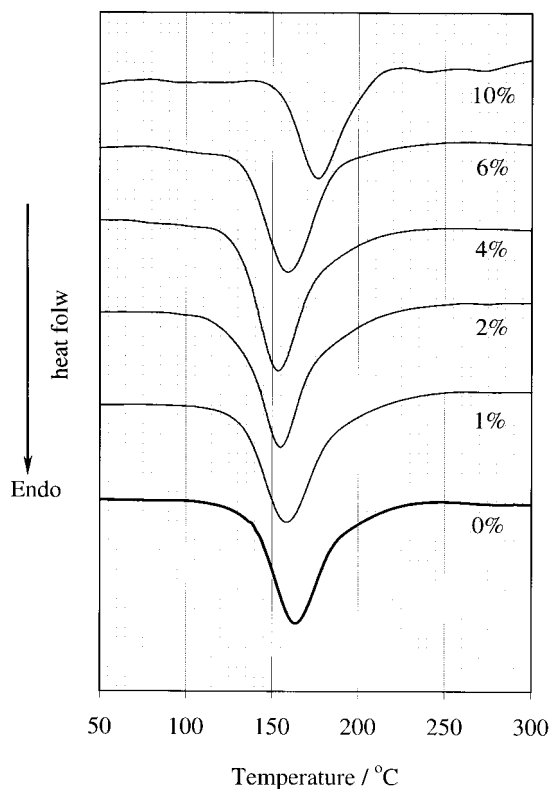


Fig. 2. DSC of BPDA/PDA poly(amide acid) with different OMMT content after drying at 60°C/6 h.

of both BPDA/PDA and PMDA/ODA poly(amide acid)s was monitored by DSC. Fig. 2 shows the DSC thermogram of BPDA/PDA poly(amide acid) in the presence of different wt.% of OMMT. Interestingly, we found that the incorporation of small amount of OMMT, up to 4% into poly(amide acid) shifted the imidization temperature to lower range. With higher OMMT content, the maxima of endotherm due to imidization shifted to higher temperature. Similarly, for Kapton type, the incorporation of 1 and 2% of OMMT shifted slightly the onset and maxima of the endotherm to lower temperature. Explanation of DSC scans of poly(amide acid) cast films is complicated because the endotherms include imidization reaction, heat of decomplexation of poly(amide acid)/solvent and residual solvent evaporation from poly(amide acid) films. From the similar results based on in-situ FT-IR [31] of the imidization of poly(amide acid)/clay, however, these results of DSC are also considered to show that the clay surface catalyzes the imidization process.

3.3. X-ray diffraction analyses of BPDA/PDA polyimide–clay hybrids

XRD patterns of BPDA/PDA polyimide–clay hybrids with different clay contents are shown in Fig. 3. The peak observed in OMMT at $2\theta = 4.83^\circ$ ($d = 1.83$ nm) corresponding to the basal spacing of OMMT has disappeared

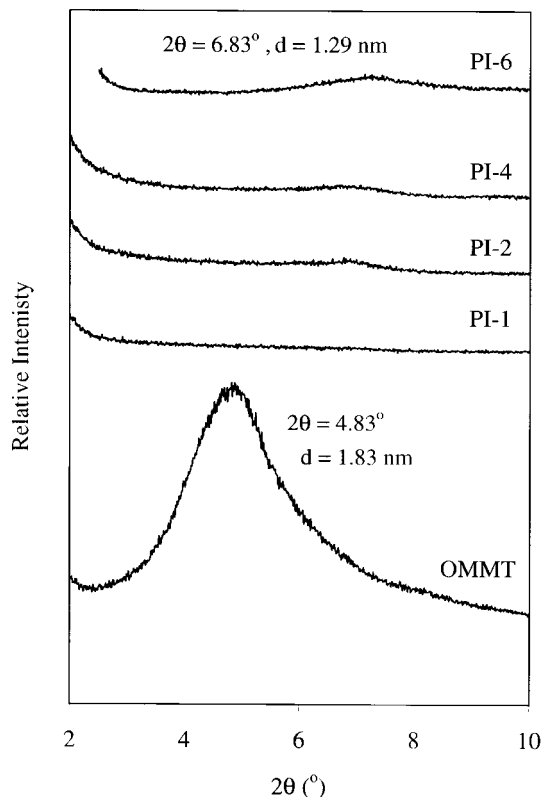


Fig. 3. XRD patterns of OMMT and BPDA/PDA–clay nanocomposite with various OMMT contents.

in the hybrids, suggesting the disorder and loss of structure regularity of the clay layers. Thus, the clay tactoids are considered to be exfoliated and the 0.96 nm-thick clay layers are dispersed at the molecular level into polyimide. However, with the increase of the OMMT loading more than 2%, the hybrids show a slight peak at ca. $2\theta = 6.83^\circ$

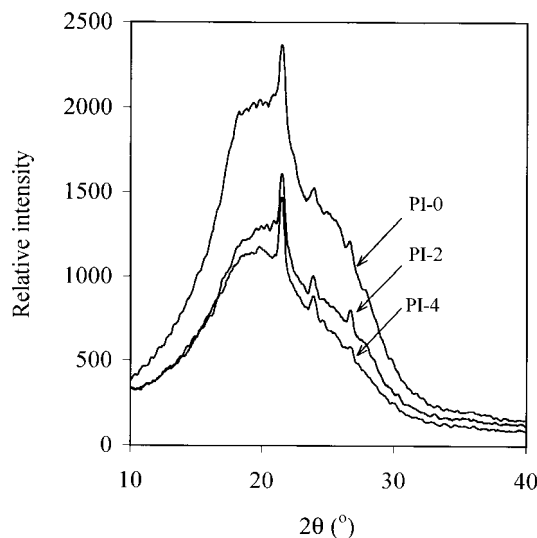


Fig. 4. XRD patterns of BPDA/PDA–clay nanocomposite with various OMMT contents.

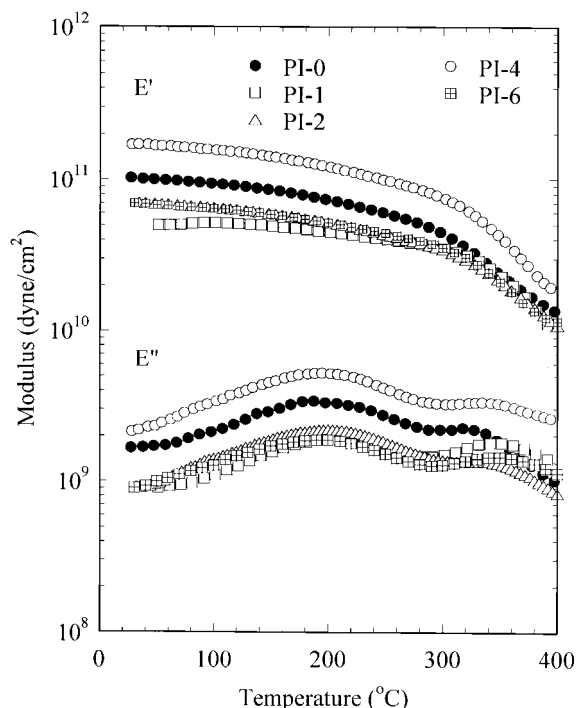


Fig. 5. Dynamic mechanical properties of BPDA/PDA–clay nanocomposites films with various OMMT contents.

($d = 1.29$ nm) suggesting that a small part of OMMT is not dispersed in the molecular level [27].

Further XRD studies for polyimide and the nanocomposites based on BPDA/PDA have been performed.

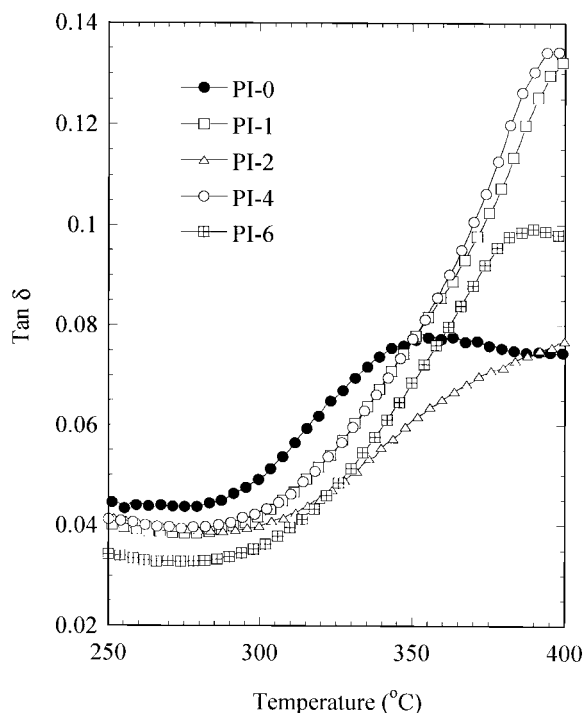


Fig. 6. $\tan \delta$ of BPDA/PDA–clay nanocomposites films with various OMMT contents.

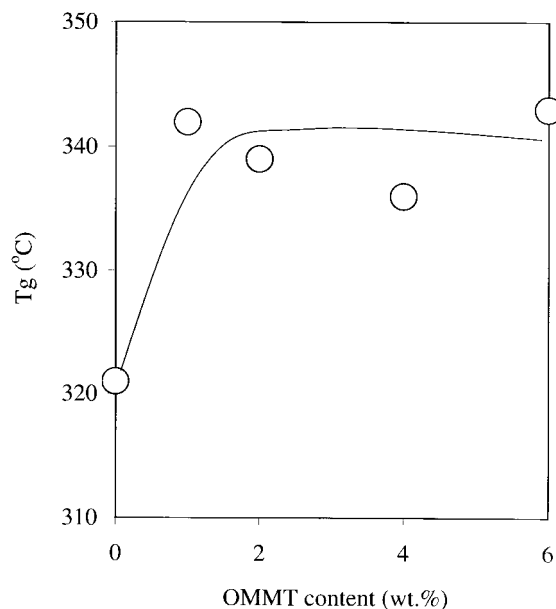


Fig. 7. Effect of the clay content on the T_g from the maxima of E'' of the BPDA/PDA–clay nanocomposites.

As shown in Fig. 4, the degree of crystallinity of BPDA/PDA slightly decreased by the inclusion of the clay nanolayers, which led to the loss of the characteristic high degree of chain orientation of BPDA/PDA.

3.4. Viscoelastic properties of BPDA/PDA polyimide–clay nanocomposites

Dynamic mechanical analysis (DMA) for the PI–clay nanocomposites was carried out to see the effect of the clay nanolayers on the thermomechanical properties of polyimide films. The storage modulus (E') and loss modulus (E'') with various clay contents are shown in Fig. 5, and the values of $\tan \delta$ are shown in Fig. 6. A small decrease in the storage modulus was observed around T_g in Fig. 5, which is typical for rigid rod polyimide. Fig. 7 shows the effect of the clay content on the T_g from the maxima of E'' curves. It was confirmed that the T_g s increased with the increase of the clay

Table 1
Effect of clay content on the tensile properties of PMDA/ODA and BPDA/PDA

PI type	Clay content (%)	E (GPa)	σ (MPa)	Elongation (%)
PMDA/ODA	0	2.7	90	30
	1	3.9	87	8
	2	5.7	69	2
	3	5.2	40	0.9
BPDA/PDA	0	8.5	192	28
	1	10.1	244	18
	2	12.1	206	8
	4	10.4	185	6

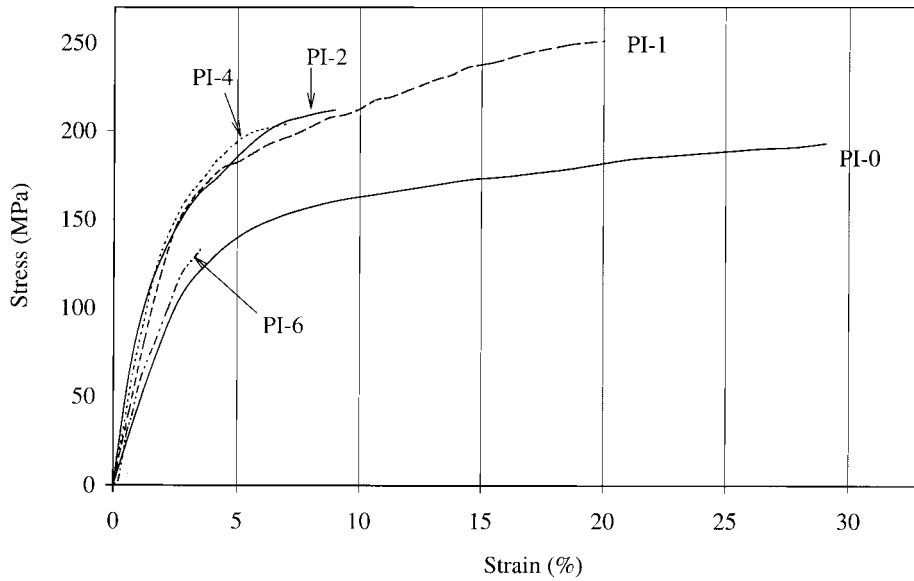


Fig. 8. Stress–strain curves of BPDA/PDA–clay nanocomposite films with various OMMT contents.

content: T_g s were 321, 342, 330, 336 and 343°C at the clay content of 0, 1, 2, 4 and 6 wt.%, respectively. The $\tan \delta$ values in Fig. 6 also show that the T_g s increased above 400°C with addition of 1% of clay. Since the glass transition process is related to the molecular motion, the T_g is considered to be affected by molecular packing, chain rigidity and linearity [32]. The increase in the T_g s of the

nanocomposites in comparison with the original polyimide can be attributed to maximizing the adhesion between the polymer and layered silicate surfaces because of the nanometer size which restricts segmental motion near

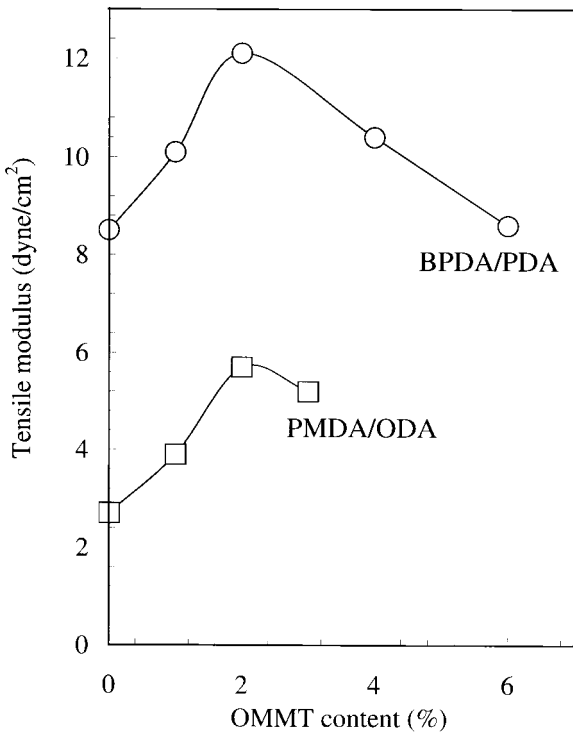


Fig. 9. Effect of clay content on the tensile modulus of the nanocomposites.

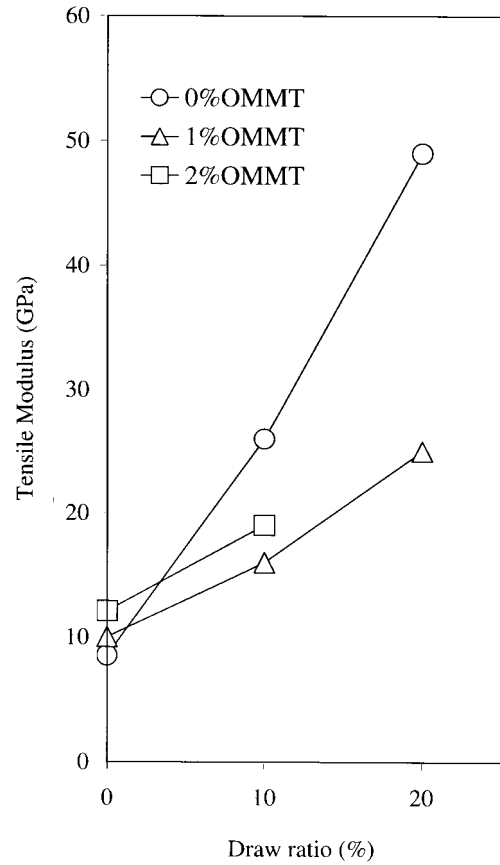


Fig. 10. Effect of draw ratio on the tensile modulus of BPDA/PDA–clay nanocomposite films.

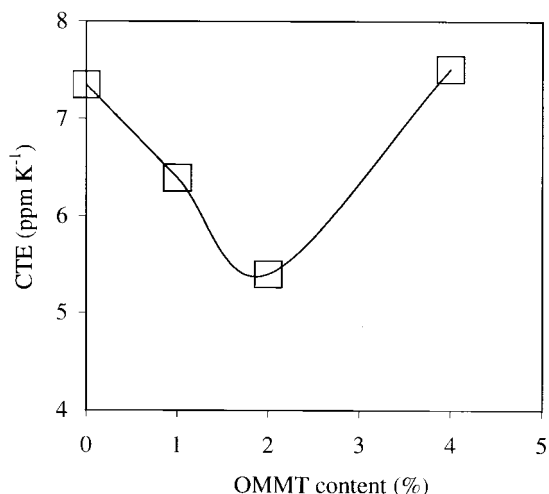


Fig. 11. Effect of clay content on the CTE of BPDA/PDA-clay nanocomposite films.

the organic inorganic interface which is a typical effect for the inclusion of clay in a polymer system [13]. The T_g for PMDA/ODA polyimide is above 400°C and could not be detected.

3.5. Tensile properties of polyimide-clay hybrid films

The tensile properties of the polyimide-clay hybrid films were examined. As summarized in Table 1, there was a clear tendency that the tensile modulus increases and elongation decreases with an increase in the OMMT content.

For pristine PMDA/ODA polyimide, which was thermally treated at 350°C/15 min, the tensile modulus was 2.7 GPa. With the incorporation of 1% OMMT, the tensile modulus increased to ca. 3.9 GPa, which is ca. 44% higher than that of the original polyimide. The increase in the modulus was accompanied with 72% decrease in the elongation at break. Addition of 2% of OMMT further increased the modulus to 5.7 GPa, which is ca. 110% higher than the pristine polyimide. It was reported from the viscoelastic analyses that the storage modulus of PMDA/ODA increased up to 25% by the inclusion of clay than the pristine polyimide [29]. Thus the tensile measurements revealed that the effect of the clay is more pronounced on the tensile modulus. The pronounced increase in the tensile modulus reflects the reinforcement effect attained by the dispersion of the clay nanolayer into polyimide film. Elongation at break, on the other hand, decreased monotonously to 2%. A further increase in the clay content (3%) started to decrease the modulus and the elongation at break sharply to be ca. 1%.

Fig. 8 shows typical stress-strain curves for BPDA/PDA-clay nanocomposites. The tensile modulus of pristine BPDA/PDA film, which was thermally treated at 350°C/1 h was 8.5 GPa. With incorporation of 1% OMMT, the tensile modulus increased to be 10.1 GPa. Addition of 2% of

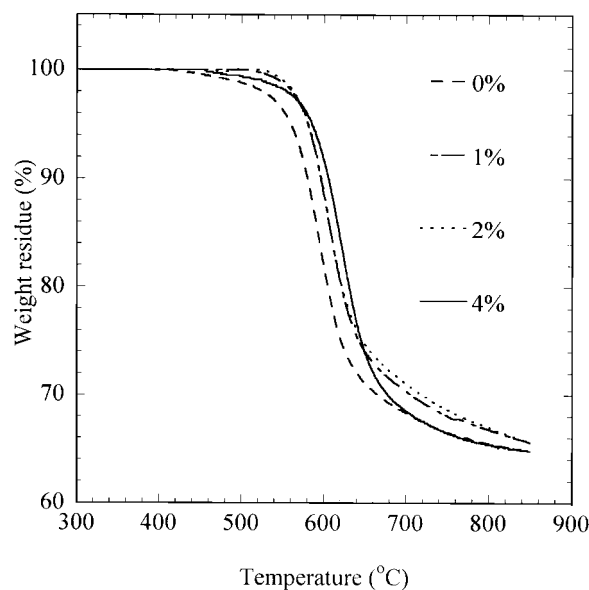


Fig. 12. TGA of BPDA/PDA-clay nanocomposites.

OMMT further increased the modulus to 12.1 GPa, which is 42% higher than the pristine polyimide. The pronounced increase in the tensile modulus reflects the reinforcement effect attained by the dispersion of the clay nanolayer into polyimide film. Elongation at break, on the other hand, decreased monotonously. Tensile strength increased with 1% of clay loading, but started to decrease at relatively low loading of clay because of the lower elongation at break. With 4% OMMT content the tensile modulus started to decrease to be 10.4 GPa. Also, the drop in the tensile properties was remarkable in the case of higher clay loading such as PI-6 (Fig. 8). This collapse of the mechanical properties can be attributed to the aggregation of the clay nanolayers.

The effect of clay loading on the tensile modulus of BPDA/PDA and also PMDA/ODA are shown in Fig. 9. The tendency of the change of modulus, increase up to 2% of loading and decrease above 2%, was the same for both BPDA/PDA and PMDA/ODDA. This means that the increase of tensile modulus is mainly based on the reinforcement effect of the dispersed clay nanolayer. The additional effect due to the chain orientation expected in case of BPDA/PDA should be minimum, if any, because of the similarity in the modulus change with PMDA/ODA.

3.6. Effect of cold drawing on BPDA/PDA polyimide-clay nanocomposites

It is well known that cold drawing of BPDA/PDA poly(amide acid) followed by imidization gives high modulus polyimide films. Thus, aiming to attain further higher modulus, the effect of cold drawing on tensile properties of the polyimide-clay hybrid films was studied. As shown in Fig. 10, the tensile modulus of the pristine

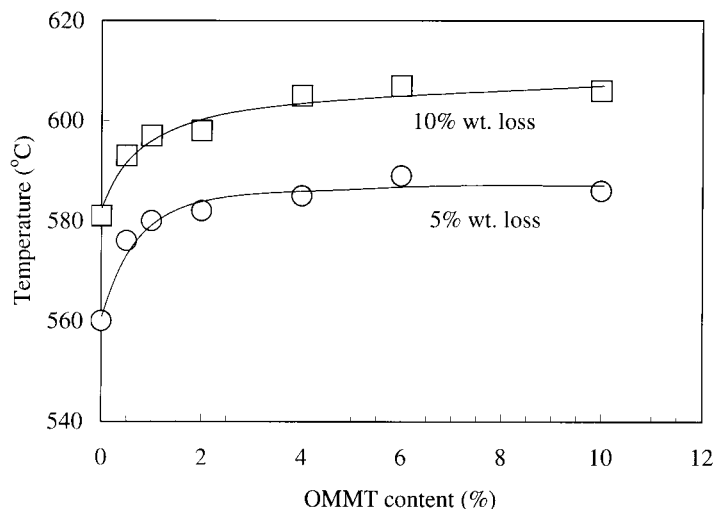


Fig. 13. Effect of clay content on the 5 and 10% decomposition of BPDA/PDA–clay nanocomposites.

BPDA/PDA polyimide increased sharply with the increase of the draw ratio. The tensile modulus increased from 8.5 GPa with 0% draw to 26 and 49 GPa with 10 and 20% draw, respectively. With inclusion of OMMT, however, the increase in the tensile modulus was not so significant as in case of pristine polyimide. As can be seen from Fig. 10, with 10% cold draw, the tensile modulus increased to be 16 and 19 GPa with inclusion of 1 and 2% clay, respectively. With 20% draw, the tensile modulus increased to be 25 GPa with 1% of clay loading. From these results, it can be stated that clay nanolayers dispersed into poly(amide acid) hindered

the mobility of the polymer molecules for crystallization during curing [31], and hence hinders the chain extension and reorientation to the draw direction in the stage of drawing of BPDA/PDA poly(amide acid).

3.7. Linear coefficient of thermal expansion of BPDA/PDA polyimide–clay hybrid films

Fig. 11 shows the effect of the inclusion of the clay nanolayers on the CTE of polyimide films. It was found that the CTE decreased from 7.35 ppm (0% clay) to be 6.39 ppm (1% clay) and 5.40 ppm K^{-1} (2% clay) with the increase of clay content up to 2% loading. The CTE, however, increased with increase of the OMMT content above 4%. This tendency is in accord with the change of the tensile modulus.

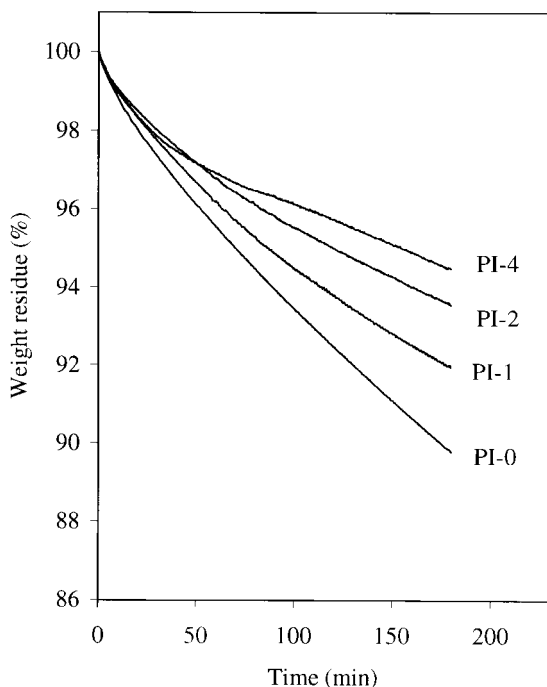


Fig. 14. Isothermal TGA of BPDA/PDA–clay nanocomposites at 500°C for 3 h.

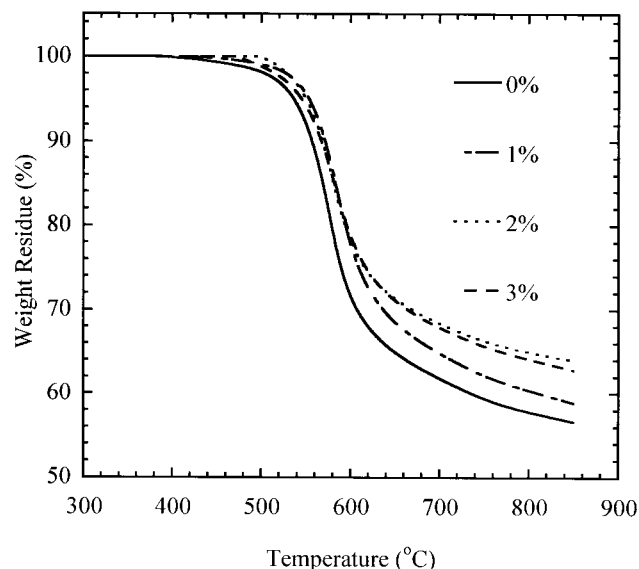


Fig. 15. TGA of PMDA/ODA–clay nanocomposites.

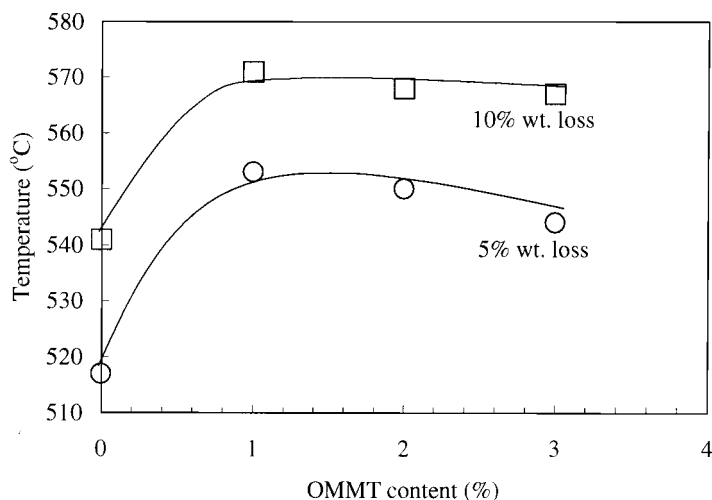


Fig. 16. Effect of clay content on the 5 and 10% decomposition of PMDA/ODA-clay nanocomposites.

3.8. Thermal properties of polyimide-clay nanocomposites

TGA were recorded for polyimide-clay nanocomposites to monitor the effect of the clay on the thermal properties. Fig. 12 shows some results of TGA in case of BPDA/PDA-clay nanocomposite. It was shown that the thermal stability increased with clay loading. The temperatures at 5 and 10% weight loss are shown in Fig. 13, which indicate that the thermal stability of the polyimide films was enhanced by the incorporation of only small amount of clay nanolayers. For example, with only 1% of OMMT content in the polyimide, the 5% decomposition temperature became higher for ca. 20°C than the corresponding pristine polyimide. Above 4% loading, the effect of clay was almost constant, probably because of the aggregation of the additional clay.

The initial decomposition of fully aromatic polyimide like BPDA/PDA is accompanied by the volatilization of carbon dioxide [33]. Therefore, the presence of clay nanolayers dispersed homogeneously into the polyimide film hinders the permeability of volatile degradation products out from the material. Fig. 14 shows the isothermal TGA for polyimide-clay at 500°C for 3 h. As clearly seen, the nanocomposites show a delayed decomposition compared with the pristine polyimide due to the homogeneous distribution of the silicate sheets which increase the total path of the volatile gases out of the film in compare with pristine polyimide.

For Kapton type polyimide, the incorporation of the clay nanolayers also enhanced the thermal stability. Fig. 15 shows the TGA traces of PMDA/ODA-clay nanocomposites and the temperatures at 5 and 10% weight loss are summarized in Fig. 16. As shown in Fig. 16, the improvement in the thermal stability was achieved by the incorporation of only 1% clay.

4. Conclusions

Polyimide-clay nanocomposites based on BPDA/PDA and PMDA/ODA polyimide with montmorillonite have the following characteristics:

1. The tensile modulus was enhanced by the inclusion of the clay nanolayers into the polyimide films, accompanied with a decrease in the elongation at break. The increase in the tensile modulus is almost solely to the reinforcement effect of the dispersed clay nanolayers. The effect of chain orientation was considered to be minimum, if any.
2. T_g s of the nanocomposites were higher than that of the pristine polyimides.
3. The CTE of BPDA/PDA decreased with the incorporation of OMMT up to 2% loading.
4. The BPDA/PDA and PMDA/ODA nanocomposites have higher thermal stability when compared to pristine polyimides.

Generally, at 2% of clay loading, the polyimide-clay nanocomposites showed the best balance in properties concerning the modulus, T_g , CTE and thermal stability due to the homogeneous dispersion of the clay.

Acknowledgements

We deeply appreciate to Dr Rikio Yokota of Institute of Space and Astronautical Science, Japan, and Mr Syougo Yamamoto of Nihon University for their kindness in measuring the CTE.

References

- [1] Jang BZ. *Compos Sci Technol* 1992;44:333.

- [2] Sohn JE. *J Adhes* 1985;19:15.
- [3] Novak BM. *Adv Mater* 1993;5:422.
- [4] Frisch HL, Mark JE. *Chem Mater* 1996;8:1735.
- [5] Giannelis EP. In: Mann S, editor. *Biomimetic mater chem*. New York: VCH, 1996 (p. 337).
- [6] Giannelis EP. *Adv Mater* 1996;8:29.
- [7] Moet A, Akelah A, Salahuddin N, Hiltner A, Baer E. *Mater Res Symp Proc* 1994;351:163.
- [8] Burnside S, Giannelis EP. *Chem Mater* 1995;7:1597.
- [9] Usuki A, Kawasumi M, Kojima Y, Okada A, Kurauchi T, Kamigaito O. *J Mater Res* 1993;8:1174.
- [10] Mehrotra V, Giannelis EP. *Solid State Ionics* 1992;51:115.
- [11] Lan T, Kaviratna PD, Pinnavaia TJ. *Chem Mater* 1995;7:2144.
- [12] Akelah A, Kelly P, Qutubuddin S, Moet A. *Clay Miner* 1994;29:169.
- [13] Agag A, Takeichi T. *Polymer* 2000;41:7083.
- [14] Massam J, Pinnavaia TJ. *Mater Res Soc Symp Proc* 1998;520:223.
- [15] Shia D, Hui CY, Burnside SD, Giannelis EP. *Polym Comp* 1998;19:608.
- [16] King FA, King JJ. *Engineering thermoplastics*. New York: Marcel Dekker, 1985 (p. 351).
- [17] Ghosh KL, Mittal KL. *Polyimides, fundamentals and applications*. New York: Marcel Dekker, 1996.
- [18] Soane D, Martynenko Z. *Polymers in microelectronics: fundamentals and applications*. Amsterdam: Elsevier, 1989.
- [19] Kochi M, Uruji T, Iizuka T, Mita I, Yokota R. *J Polym Sci, Part C: Polym Lett* 1987;25:441.
- [20] Kochi M, Yokota R, Iizuka T, Mita I. *J Polym Sci, Part B: Polym Phys* 1990;28:2463.
- [21] Takeichi T, Takahashi N, Yokota R. *J Polym Sci, Part A: Polym Chem* 1994;32:167.
- [22] Takeichi T, Miyaguchi N, Yokota R. *High Perform Polym* 1995;7:357.
- [23] Takeichi T, Tanikawa M, Zuo M. *J Polym Sci, Part A: Polym Chem* 1997;35:2395.
- [24] Takeichi T, Endo Y, Kaburagi Y, Hishiyama Y, Inagaki M. *J Appl Polym Sci* 1996;61:1571.
- [25] Takeichi T, Endo Y, Kaburagi Y, Hishiyama Y, Inagaki M. *J Appl Polym Sci* 1998;68:1613.
- [26] Takeichi T, Eguch Y, Kaburagi Y, Hishiyama Y, Inagaki M. *Carbon* 1999;37:569.
- [27] Yano K, Usuki A, Okada A, Kurauchi T, Kamigaito O. *J Polym Sci, Part A: Polym Chem* 1993;31:2493.
- [28] Lan T, Kaviratna PD, Pinnavaia TJ. *Chem Mater* 1994;6:573.
- [29] Yano K, Usuki A, Okada A. *J Polym Sci, Part A: Polym Chem* 1997;35:2289.
- [30] Yang Y, Zhu Z, Yin J, Wang X, Qi Z. *Polymer* 1999;40:4407.
- [31] Tyan H, Liu Y, Wei K. *Polymer* 1999;40:4877.
- [32] Li F, Ge J, Honigfort P, Fang S, Chen J-C, Harris F, Cheng S. *Polymer* 1999;40:4987.
- [33] Inagaki M, Takeichi T, Hishiyama Y, Oberlin A. *Chem Phys Carbon* 1999;26:245.